

FUSION RESEARCH CENTER

RECEIVED
SEP 01 1993
OSTI

DOE/ER-53266-45

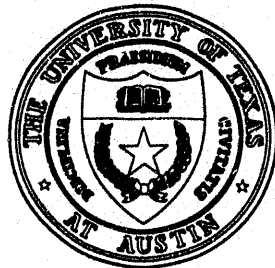
FRCR #436

Neoclassical Kinetic Theory Near an X-Point: Plateau Regime

E.R. SOLANO AND R.D. HAZELTINE
Fusion Research Center
The University of Texas at Austin
Austin, Texas 78712

August 1993

THE UNIVERSITY OF TEXAS



Austin, Texas

MASTER

DISTRIBUTION OF THIS DOCUMENT IS UNLIMITED

NEOCLASSICAL KINETIC THEORY NEAR AN X-POINT: PLATEAU REGIME.

E. R. SOLANO and R. D. HAZELTINE[†],

Fusion Research Center, Institute for Fusion Studies[†], The University of Texas at Austin..

Traditionally, neoclassical transport calculations ignore poloidal variation of the poloidal magnetic field. Near an X-point of the confining field of a diverted plasma, the poloidal field is small, causing guiding centers to linger at that poloidal position. We study how neoclassical transport is affected by this differential shaping. The problem is solved in general in the plateau regime, and a model poloidal flux function with an X-point is utilized as an analytic example to show that the plateau diffusion coefficient can change considerably (factor of 2 reduction). Ion poloidal rotation is proportional to the local value of \vec{B}_{pol} , but otherwise it is not strongly affected by shaping.

1. Introduction

Neoclassical theory is by now a well developed subject. Nevertheless, as experimental research in plasma confinement advances, some old questions need to be revisited. One of these questions arises in connection with diverted plasmas. In its most naive formulation it can be stated as follows: as the safety factor near a separatrix approaches infinity, what happens to neoclassical predictions? The naive reply is that since neoclassical transport is proportional to the safety factor, neoclassical transport near a separatrix would be very large. We show in this paper that this is not the case.

Neoclassical transport coefficients in plateau regime can be calculated taking into account the differential plasma shaping associated with the vicinity of an X-point. Our method does not allow studying the separatrix itself, since our change of variable becomes singular at the X-point. Outside the separatrix the transport issue is complicated by loss cone effects, hence we study a region approaching the separatrix, but inside it: the poloidal variation of the poloidal magnetic field is there, but not the X-point.

First of all we briefly review the definition of the collisionality regimes and choice of coordinates in section 2. In section 3 we solve the drift kinetic equation and compute the distribution function. Transport coefficients are defined and calculated in section 4. Rotation rates are calculated in section 5, while a particular analytical example is considered in section 6. Conclusions and comments are presented in section 7.

2. Drift kinetic equations, choice of coordinates and collisionality.

In (ξ, v) velocity coordinates, the drift kinetic equations have the form¹:

$$\xi v \nabla_{\parallel} f - v(1 - \xi^2) \nabla_{\parallel} (\ln B) \frac{\partial f}{\partial \xi} - C(f) = \alpha_n f_0 \quad (1)$$

Here v is the velocity of the guiding center, ξ is the pitch angle ($\xi = v_{\parallel}/v$), the subscript \parallel indicates the component of the vector parallel to the magnetic field, \vec{B} , and f_0 is the zeroth order solution to the kinetic equation, a Maxwellian distribution function, with only radial variation.

The first term in the lhs of equation (1) represents streaming of the guiding center along field lines. The second term represents the mirror effect (which, when combined with a ∇B drift on the rhs, produces banana orbits). The third term in the lhs is the Coulomb collision operator. A typical source term in the rhs would be the ∇B drift, $-v_d \cdot \nabla f_0 = \frac{mv^2}{2e} (1 + \xi^2) \frac{1}{B} \nabla_{\parallel} (\ln B) \frac{df_0}{d\chi}$. The inclusion of other source terms would lead to other transport coefficients (see Ref. 1).

Given a poloidal flux function χ , the magnetic field can be written in symmetry coordinates as $B = I \nabla \zeta + \nabla \zeta \times \nabla \chi$. Here ζ is the geometrical toroidal angle and $I = R B_t$. Note that the poloidal flux is actually $\Psi_p = 2\pi \chi$. Using a geometric poloidal angle θ (cylindrical-like coordinates centered on the magnetic axis), the drift kinetic equation with a ∇B drift source term can be written as:

$$\xi v \frac{\vec{B}_p \cdot \nabla \theta}{B} \frac{\partial f}{\partial \theta} + \frac{v}{2} (1 - \xi^2) \frac{\vec{B}_p \cdot \nabla \theta}{B} \frac{\partial \ln B}{\partial \theta} \frac{\partial f}{\partial \xi} - C(f) = \frac{mv^2}{2e} (1 + \xi^2) \frac{1}{B} \frac{\vec{B}_p \cdot \nabla \theta}{B} \frac{\partial \ln B}{\partial \theta} \frac{df_0}{d\chi} \quad (2)$$

The most natural poloidal variable is given by Θ , defined as:

$$\Theta(\theta) = \frac{1}{L_c} \int_0^\theta \frac{B d\theta}{B_p \cdot \nabla\theta}; \quad L_c = \frac{1}{2\pi} \int_0^{2\pi} \frac{B d\theta}{B_p \cdot \nabla\theta} \quad (3)$$

L_c can be best understood as a connection length.

Equation (2) can now be written as:

$$\frac{\xi v}{L_c} \frac{\partial f}{\partial \Theta} + \frac{v(1-\xi^2)}{2L_c} \frac{\partial \ln B}{\partial \Theta} \frac{\partial f}{\partial \xi} - C(f) = \frac{1}{L_c} \frac{mv^2}{2e} (1+\xi^2) \frac{1}{B} \frac{\partial \ln B}{\partial \Theta} \frac{df_0}{d\chi} \quad (4)$$

Collisionality regimes are determined by establishing which term in the lhs of the drift kinetic equation is smallest and can therefore be ignored in the lowest order approximation. In the plateau regime streaming occurs in a faster time scale than the collisions, but there is competition between the mirror force and collisions. This is resolved by adopting a large aspect ratio approximation, which decreases the mirror force and doesn't affect collisions. So the plateau regime is given by:

$$\frac{\xi v}{L_c} \frac{\partial f}{\partial \Theta} \gg C(f) \gg \frac{1}{L_c} \frac{mv^2}{2e} (1+\xi^2) \frac{1}{B} \frac{\partial \ln B}{\partial \Theta} \frac{df_0}{d\chi}$$

with the assumption of small mirror force:

$$\frac{v(1-\xi^2)}{2L_c} \frac{\partial \ln B}{\partial \Theta} \frac{\partial f}{\partial \xi} \ll C(f)$$

As the X-point is approached (or external shaping is applied), the connection length L_c increases, so for a fixed collision frequency the plasma can transition to the collisional regime if L_c becomes sufficiently large.

3. Distribution function

As mentioned above, in the large aspect ratio approximation the mirror term can be ignored in first order. To further simplify the problem, we use a Krook collision operator, $C(f) = -v f$. Collecting all the terms in the rhs that are independent of θ in \bar{S} , and using the Θ angle defined in equation (3), we have:

$$\frac{\partial f}{\partial \Theta} + \frac{v L_c}{\xi v} f = -\frac{\bar{S}}{\xi v} f_0 \frac{B_0}{B} \frac{\partial \ln B}{\partial \Theta} \frac{df_0}{d\chi} \quad (5)$$

Here B_0 is some characteristic value of the magnetic field in that flux surface. For instance it could be the flux surface averaged value of B , $B_0 = \langle B \rangle$, or it could be the total magnetic field at the axis.

Defining $\gamma = v L \partial \xi / v$, and using the integrating factor method, the solution of equation (5) is:

$$f(\Theta) = -\frac{\bar{S}}{\xi v} \frac{df_0}{d\chi} e^{-\gamma\Theta} \int e^{\gamma\Theta} \left(\frac{B_0 \ln B}{B} \frac{\partial \ln B}{\partial \Theta} \right) d\Theta =$$

$$= -\frac{\bar{S}}{\xi v} \frac{df_0}{d\chi} \sum_k \frac{s_k^1 [\gamma \sin(k\Theta) - k \cos(k\Theta)] + c_k^1 [k \sin(k\Theta) + \gamma \cos(k\Theta)]}{\gamma^2 + k^2}$$

with the Fourier coefficients:

$$\begin{Bmatrix} s_k^n \\ c_k^n \end{Bmatrix} = \oint d\Theta \left[\left(\frac{B_0}{B} \right)^n \frac{\partial \ln B}{\partial \Theta} \right] \begin{Bmatrix} \sin(k\Theta) \\ \cos(k\Theta) \end{Bmatrix} \quad (6)$$

In the plateau limit:

$$\lim_{\frac{vL}{v} \rightarrow 0} \frac{1}{\xi v} \frac{\gamma}{\gamma^2 + k^2} \rightarrow \frac{\pi}{vk} \delta(\xi) \quad \text{and} \quad \lim_{\frac{vL}{v} \rightarrow 0} \frac{1}{\xi v} \frac{k}{\gamma^2 + k^2} \rightarrow 0.$$

so,

$$f(\Theta) = \bar{S} \frac{df_0}{d\chi} \delta(\xi) \sum_k \frac{s_k^1 \sin(k\Theta) + c_k^1 \cos(k\Theta)}{k} \quad (7)$$

4) Transport coefficients (particle and heat diffusivities):

Now that we have the distribution function, fluxes and/or transport coefficients can be computed. Assuming stationary flux surfaces (the Ware pinch can be considered as a separate problem), the number of particles that cross a given flux surface per unit of time is given by:

$$\frac{dN}{dt} = \oint \frac{d\theta}{B_p \cdot \nabla \theta} \langle \Gamma \cdot \nabla \chi \rangle \quad (8)$$

with $\langle \Gamma \cdot \nabla \chi \rangle = \langle \int d^3v f_e v_{de} \cdot \nabla \chi \rangle$. Here the flux surface average is given by :

$$\langle A \rangle = \left(\oint \frac{A d\theta}{B_p \cdot \nabla \theta} \right) \left(\oint \frac{d\theta}{B_p \cdot \nabla \theta} \right)^{-1}$$

We define the particle diffusivity D as the proportionality constant between $\frac{dN}{dt}$ and $\frac{dn}{d\chi}$. The loss rate is

$$\left(\oint \frac{d\theta}{B_p \cdot \nabla \theta} \right) \langle \Gamma \cdot \nabla \chi \rangle = - \frac{\sqrt{\pi}}{4} \left(\frac{m v_{the}}{e B_0} \right)^2 \frac{I^2}{B_0} \left(\sum_k \frac{s_k^1 s_k^2 + c_k^1 c_k^2}{k^2} \right) \left[\frac{1}{n_e} \frac{dn_e}{d\chi} + \dots \right] n_e v_{th}$$

Hence, the diffusivity is

$$D = - \frac{\sqrt{\pi}}{4} \left(\frac{m v_{the}}{e B_0} \right)^2 \frac{I^2}{B_0} \left(\sum_k \frac{s_k^1 s_k^2 + c_k^1 c_k^2}{k^2} \right) v_{the} \quad (9)$$

In a circular plasma (large aspect ratio approximation) $s_1^1 = s_1^2 = \frac{a}{R_0}$, and all the other coefficients are higher order. So the ratio of the diffusivities in a shaped plasma and a circular plasma (with the same cross sectional area, I , plasma current I_p , B_0 , R_0 , T_e) is

$$R_D = \left(\frac{R_0}{a} \right)^2 \left(\sum_k \frac{s_k^1 s_k^2 + c_k^1 c_k^2}{k^2} \right) \quad (10)$$

Other transport coefficients will be similarly modified by the poloidal variation of the magnetic field. For instance, particle diffusivity, electron and ion heat diffusivity will all be modified in exactly the same manner.

Note that the transport coefficients we calculated are not proportional to the "poloidal Larmor radius" (ρ_{pol}). Nothing spectacular happens to them as the separatrix is approached (they may become harder to calculate). Neither is the particle (or heat) loss, which is proportional to $dn/d\chi$ (or $dT/d\chi$). At the separatrix there is no special singularity associated with the χ derivatives of density or temperature. On the other hand, there is a " I_p scaling" of the confinement time. If we choose the normalized flux as our flux label

$$\frac{dn}{d\chi} = \frac{1}{\chi_0} \frac{dn}{d\chi/\chi_0}$$

the loss rate is inversely proportional to the poloidal flux at the last closed flux surface. For a given plasma current I_p , the value of χ_0 depends on the plasma shape, size and current profile. It can either be larger or smaller than in the

equivalent circular case. But for constant shape χ_0 will always increase with plasma current. This provides the familiar I_p scaling of confinement, brought about by the flux surface average necessary to consider transport as a diffusive process. In that sense there is a "rho pol scaling" of the confinement time.

Here it should be pointed out that a calculation of plateau transport very similar to the one presented so far was undertaken by Meier, Hirshman and Sigmar³. Its results are mentioned in Ref. 2, but the original paper was never published. Our results are somewhat more complete in the plasma shape description and in the analysis of their implications for a diverted plasma, although our collision operator is simpler, since the full operator is not necessary to compute plateau transport.

5) Ion rotation

The drift kinetic equation is invariant under the transformation $f \rightarrow f + f_d$, with $f_d = (2v_{||} \cdot U_{||} / v_{th}^2) f_M$ (a displaced Maxwellian).

To resolve the degenerate problem the mirror force term (next order) needs to be included in the ion DKE :

$$v_{||} \nabla g - C(g) = -v_{Di} \cdot \nabla f_0 - M(f_d)$$

Imposing flux surface averaged parallel momentum conservation:

$$\left\langle \int d^3v \xi v \left[\xi v \nabla_{||} g - M(g) - C(g) - v_{Di} \cdot \nabla f_0 \right] \right\rangle = 0.$$

allows evaluating the actual ion parallel rotation velocity, $U_{||}$:

$$U_{||} = \frac{T_i}{eB} \left[\frac{1}{p_i} \frac{dp_i}{d\chi} + \frac{e}{T_i} \frac{d\Phi}{d\chi} + \frac{1}{2} \frac{1}{T_i} \frac{dT_i}{d\chi} \frac{B^2}{B_0^2} U_D \right] \quad (11)$$

with:

$$U_D = \frac{\left(\sum_k \frac{s_k^1 s_k^1 + c_k^1 c_k^1}{k^2} \right)}{\left(\sum_k \frac{s_k^1 s_k^{-1} + c_k^1 c_k^{-1}}{k^2} \right)} \quad (12)$$

In a large aspect ratio case the Fourier components are all almost equal, so U_D is very similar to 1.

Like the transport coefficients, the parallel rotation is proportional to radial gradients measured with the χ flux label. In that sense it is "proportional to ρ_{pol} ": if the amount of poloidal flux inside a given surface is small, the parallel rotation will be large.

Adding the poloidal components of perpendicular and parallel rotation, we have the poloidal rotation:

$$\vec{U}_{pol} = -\frac{1}{2} \left| \frac{1}{e} \frac{dT_i}{d\chi} \right| \frac{\vec{B}_{pol}}{B_0^2} U_D \quad (13)$$

Note that the local value of the poloidal rotation is proportional to the local value of the poloidal magnetic field, strongly affected by shaping. It will be approach zero near the X-point. On the other hand, the amount of poloidal flux inside a given surface is canceled by the χ factor contained inside \vec{B}_{pol} . In that sense, the poloidal rotation is "proportional to ρ_{tor} ".

6. Example:

As a model of a poloidal flux function with a separatrix, we have chosen:

$$\chi(r, \theta) = \chi_0 \left(\frac{r}{b} \right)^2 \left[2 + \left(\frac{r}{b} \right)^2 \cos(2\theta) \right] = \chi_0 \left[\left(\frac{x}{b} \right)^2 + \left(\frac{y}{b} \right)^2 \right] \left[2 + \left(\frac{x}{b} \right)^2 - \left(\frac{y}{b} \right)^2 \right] \quad (14)$$

Here, r is the polar radial coordinate, and in a flux surface it is a function of θ . We have chosen this function because it is easy to obtain approximate analytic expressions for $r(\chi, \theta)$ and $\Theta(\chi, \theta)$ in a large aspect ratio.

A plot of the contours of χ , its $q(\sqrt{\chi})$ profile and $\vec{B}_p \cdot \nabla \theta / B$ vs. θ at $\chi/\chi_0 = .9$ is shown in Figure 1. Notice that $\vec{B}_p \cdot \nabla \theta / B$ is small near the X-points, but it is larger far away from them ($\int \vec{B}_p dl = \mu_0 I_p$ will ensure that in some average sense the poloidal field can not decrease everywhere for fixed plasma current).

For the flux function described in equation (14) the Fourier series only have sine terms, and they converge very quickly. For a "large aspect ratio

TEXT-like tokamak* ($a=.27$ m, $I_0= B_{t0}R_0= 2$ T-m, $R_0= 2$ m) the values of the Fourier coefficients at $\chi/\chi_0= .9$ are shown in Table 1. The plasma current, $I_p= 61$ kA, was chosen to produce $q(a)= 3$ in the case of an equivalent circular plasma. It determines the value of χ_0 .

The computation of the diffusivity ratio R_D (equation 14) and of the rotation shape coefficient U_D in this case gives:

$$R_D= .59$$

$$U_D= .99$$

So it is clear that shaping can significantly reduce the particle and heat diffusivities. The poloidal rotation rate, on the other hand, is almost only affected by the different local values of \vec{B}_{pol} .

7. Conclusions and comments:

All other things being equal, the plateau -collisional and banana-plateau transitions can happen at different collision frequencies if the connection length is modified. As L_c increases, the plasma enters a higher collisionality regime, for fixed collision frequency.

The neoclassical particle and heat transport coefficients in plateau regime have been calculated and it was shown in a particular case that they can be reduced by a factor of 2 by plasma shaping. We speculate that they could also be increased, for instance by placing the X-point in the outside mid-plane, thereby increasing the ∇B drift. The particle and heat loss rates are modified in the same manner, if $dn/d\chi$ is the same. They do not increase with the connection length.

The poloidal rotation speed is proportional to \vec{B}_{pol} , so it becomes small near the X-point. Shaping can also modify its overall magnitude, but the effect is small in large aspect ratio tokamaks.

Other collisionality regimes are also affected by the proximity of an X-point. In the collisional regime previous results^{4,5,2} are applicable, so we didn't readdress the problem. Qualitatively, it is clear that collisionless transport will also be affected by shaping or an X-point. The trapped population can be

reduced/increased by placing the X-point on the inner/outer side of the tokamak. We expect modifications to banana regime transport to be of the same order as they are in plateau regime (~ factor of 2).

Acknowledgments:

We would like to acknowledge valuable discussions with Bill Rowan, Sveta Sasharina, Prashant Valanju, Allan Wootton and Peter Yushmanov. We are grateful to Dieter Sigmar for providing us with a copy of Reference 3., and for his encouragement. This work has been supported by USDOE under grants DE-FG05-88ER-53266 and DE-FG05-88ER-532088.

References:

- ¹ F. L. Hinton, R. D. Hazeltine, Rev. Mod. Phys. 48, 239 (1976).
- ² S. P. Hirshman, D. J. Sigmar, Nucl. Fus. 21, 1079 (1981).
- ³ H. K. Meier, S. P. Hirshman, D. J. Sigmar, Oak Ridge National Lab Report ORNL -TM -7584 (1980).
- ⁴ R. D. Hazeltine, F. L. Hinton, Phys. Fluids 16, 1883 (1973).
- ⁵ R. D. Hazeltine, Phys. Fluids 17, 961 (1974).

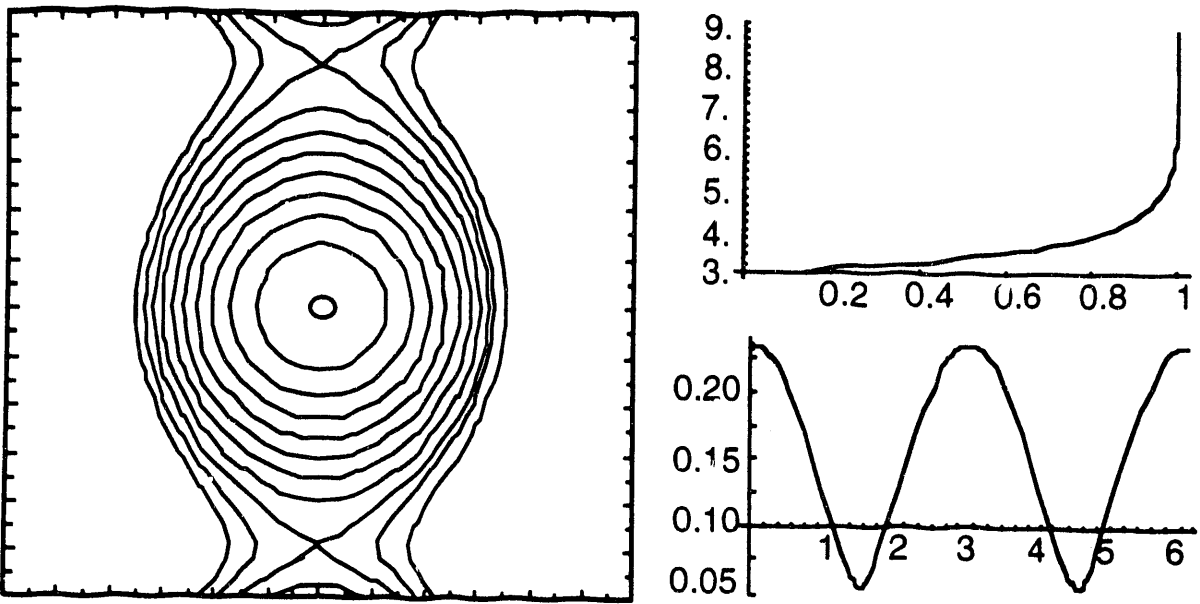


Fig 1.: Flux contours, $q(\sqrt{\chi/\chi_0})$ profile and $\vec{B}_p \cdot \nabla\theta/B$ vs θ for the example case.

k	1	2	3	4
s_k^1	.103	.003	.043	.001
s_k^2	.103	.004	.042	.002
s_k^{-1}	.104	-.016	.045	-.008

Table 1: Values of the Fourier sine series coefficients described in equation (6) for the flux function of equation (14).

DISCLAIMER

This report was prepared as an account of work sponsored by an agency of the United States Government. Neither the United States Government nor any agency thereof, nor any of their employees, makes any warranty, express or implied, or assumes any legal liability or responsibility for the accuracy, completeness, or usefulness of any information, apparatus, product, or process disclosed, or represents that its use would not infringe privately owned rights. Reference herein to any specific commercial product, process, or service by trade name, trademark, manufacturer, or otherwise does not necessarily constitute or imply its endorsement, recommendation, or favoring by the United States Government or any agency thereof. The views and opinions of authors expressed herein do not necessarily state or reflect those of the United States Government or any agency thereof.

END

**DATE
FILMED**

10 / 25 / 93